Zeolites | Hot Paper

Influence of Intracrystalline Ionic Strength in MFI Zeolites on Aqueous Phase Dehydration of Methylcyclohexanols

Lara Milaković⁺, Peter H. Hintermeier⁺, Yue Liu, Eszter Baráth,* and Johannes A. Lercher*

Abstract: The impact of the concentration of hydrated hydronium ions and in turn of the local ionic strength in MFI zeolites has been investigated for the aqueous phase dehydration of 4-methylcyclohexanol (E1 mechanism) and cis-2-methylcyclohexanol (E2 mechanism). The E2 pathway with the latter alcohol led to a 2.5-fold higher activity. The catalytic activity normalized to the hydronium ions (turnover frequency, TOF) passed through a pronounced maximum, which is attributed to the increasing excess chemical potential of the alcohols in the pores, increasing in parallel with the ionic strength and the additional work caused by repulsive interactions and charge separation induced by the bulky alcohols. While the maximum in rate observed is invariant with the mechanism or substitution, the reaction pathway is influencing the activation parameters differently.

Zeolitic Brønsted acid sites (BAS) are generated by substitution of metal cations with a $3+$ charge to the framework Si^{4+}-oxygen tetrahedra. Although often denoted as a "proton", i.e., a H^+, the acid site is intrinsically a charge-neutral hydroxyl group in which the hydrogen atom is covalently bonded to the oxygen bridging between Si and Al based tetrahedra. In gas phase, BAS of a specific type of zeolite tend to have a similar acid strength and, therefore, act catalytically similarly on reactive substrates.[1] Stronger deviations occur, if the zeolite has pronounced differences in the Al locations, a substantial concentration of extra-framework Al, and Al concentrations that lead to substantial concentration of aluminum as next nearest neighbors.[2–5]

[*] L. Milaković,[+] Dr. P. H. Hintermeier,[+] Dr. Y. Liu, Dr. E. Baráth, Prof. Dr. J. A. Lercher
Department of Chemistry and Catalysis Research Center
Technische Universität München
Lichtenbergstraβe 4, 85748 Garching (Germany)
E-mail: eszter.barath@tum.de
        johannes.lercher@ch.tum.de

Dr. P. H. Hintermeier,[+] Prof. Dr. J. A. Lercher
Institute for Integrated Catalysis
Pacific Northwest National Laboratory
902 Battelle Boulevard, Richland, WA 99352 (USA)

[+] These authors contributed equally to this work.

Supporting information and the ORCID identification number(s) for the author(s) of this article can be found under:
https://doi.org/10.1002/anie.202107947.

Zeolites tend to be unstable in aqueous phase at elevated temperatures.[6] Recent studies showed, however, that the zeolite frameworks tend to be stable for a prolonged time in aqueous phase, if temperatures do not exceed 180 °C.[7] The suitability of the solid acids as catalyst for converting oxo-functionalized molecules derived from renewable resources, has led to a quite intense exploration of molecular sieves in such aqueous environment.[8]

It has been shown that in presence of water the covalently bound OH group balancing the charge of aluminum–oxygen tetrahedron is deprotonated, forming a hydrated hydronium ion (abbreviated as $H_3O^+_{hydr.}$).[9] The hydration shell forms a fluxional, positively charged cluster that remains close to the anion in the zeolite lattice. The size of the cluster depends on the micropore size of the zeolite. We have shown its composition to be $H^+(H_2O)_8$ in MFI, creating an empty void between these clusters.[10] Sorbed organic substrates, e.g., cyclohexanol or phenol, may be sorbed in these voids between neighboring hydrated hydronium ions.[10, 11]

This transforms the zeolite pores in water into a strongly ionic environment, with the concentration of hydronium ions in the volume of the zeolite pores, approximating liquids with high ionic strength. We have shown that a high intracrystalline ionic strength induces a strong non-ideality and destabilizes a sorbed organic substrate by increasing its excess chemical potential compared to a zeolite pore without acid sites, similarly to the increase in the excess chemical potential as the ionic strength of an electrolyte solution is increased. The intracrystalline ionic strength increases proportionally to the H_3O^+ concentration, leading to a monotonic increase of the standard free energy of adsorption of nonpolar or less polar substrates in zeolite pores.[12]

Using cyclohexanol dehydration to cyclohexene catalyzed by MFI and BEA in water it was shown recently that the ionic environment in zeolite crystallites stabilizes the cationic transition state, thus, decreasing the reaction barrier and enhancing the reaction rate.[12] This provides a new path to influence the catalytic activity of Brønsted acidic zeolites.

Herein, we investigate, how the intracrystalline ionic strength influences the reaction rate in the dehydration of substituted cyclic alcohols, independent of the reaction mechanism (E1 vs. E2 elimination) respond to the ionic strength and whether variations in the steric hindrance changes the impact of ionic strength.

Two isomers of methylcyclohexanol were chosen for the study, i.e., 4-methylcyclohexanol (4-McyOH) and *cis*-2-methylcyclohexanol (*cis*-2-McyOH). The former is shown to dehydrate via an E1 mechanism and can access to all micropore space in MFI channels, while the latter dehydrates via an E2 mechanism[13] and can only access part of the MFI

Table 1: Characterization of the investigated MFI zeolites, measured kinetic (150°C) and activation parameters of 4-McyOH dehydration over MFI zeolites.

| Entry	Zeolite	V_{micro} [cm³ g⁻¹]	Unit cell volume [Å³][a]	c (BAS) [mmol g$_{MFI}$⁻¹]	Ionic strength [mol L⁻¹]	TOF [s⁻¹]	$\Delta G^{o\ddagger}$ [kJ mol⁻¹]	$\Delta H^{o\ddagger}$ [kJ mol⁻¹]	$\Delta S^{o\ddagger}$ [J mol⁻¹ K⁻¹]
1	MFI-193	0.10	5374.4	0.09	0.89	0.009	121±2	149±1	66±3
2	MFI-90[b]	0.13	5376.8	0.15	1.12	0.024	–	–	–
3	MFI-60	0.15	5376.8	0.23	1.51	0.030	117±6	143±3	60±6
4	MFI-45	0.12	5376.7	0.36	3.00	0.015	120±2	145±1	59±3
5	MFI-40	0.15	5372.8	0.31	2.07	0.031	117±9	141±5	56±10
6	MFI-15	0.18	5380.9	0.86	4.92	0.005	124±7	157±4	77±8
7	MFI-12	0.18	5377.3	1.14	6.44	0.004	124±6	153±3	68±7

[a] Derived from XRD (lattice parameters a,b,c in Supporting Information, Table S1). [b] Experiment conducted only at 150°C.

micropore space due to its bulkiness. The comparison of the dehydration rates of the two substrates catalyzed by a series of MFI zeolites with varying BAS concentrations allows to address the role of steric challenges and of the nature of the transition state.

The most important physicochemical properties of the zeolites are compiled in Table 1 (additional in Supporting Information, Table S1). With increasing Si/Al ratio, the BAS (and hence $H_3O^+_{hydr.}$) decreased from 1.14 to 0.09 mmol g⁻¹. The micropore volumes (V_{mirco}) were found to be low for MFI with high Si/Al ratio and tended to increase with decreasing Si/Al ratio. The calculated unit cell volumes in Table 1 show that the unit cell does not change significantly across all samples studied. Thus, the differences in V_{mirco} are tentatively attributed to (presumably silica) debris in the pores. By normalizing the BAS concentration (forming quantitatively hydrated hydronium ions) to the micropore volumes the intracrystalline ionic strength was calculated to range from 0.89 to 6.44 mol L⁻¹ (*Ionic strength* $= c(BAS) V_{micro}^{-1}$).

Previous investigations have established that *trans*-2-McyOH and 4-McyOH (*cis/trans*) dehydrate via carbenium ion intermediates following an E1 mechanism.[13] 4-McyOH is thereby predominately dehydrated to 4-methylcyclohexene (4-MCH), which represents the Hofmann-product (Scheme 1).[13,14]

In contrast, the concerted E2 mechanism was concluded to dominate in the dehydration of *cis*-2-McyOH, which almost exclusively resulted in the formation of the Saytzeff-product 1-methylcyclohexene (1-MCH) (Scheme 1).[13,15] The *cis* isomer shows a 30 kJ mol⁻¹ lower activation barrier than the *trans* isomer and, therefore, is converted preferentially in
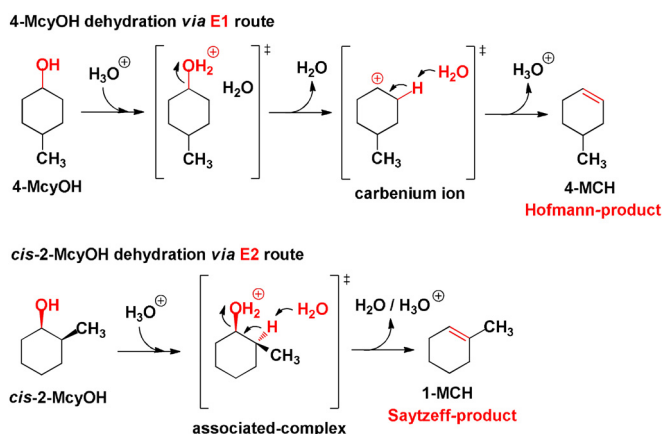
Scheme 1. Dehydration mechanism of 4-McyOH (E1) and *cis*-2-McyOH (E2).[13]

a racemic mixture of both isomers. The reaction order in 2- and 4-McyOH was zero for MFI zeolites; consequently, it is assumed that the measured activation parameters are representing intrinsic values, i.e., the energy difference between transition state and sorbed substrate (Supporting Information, Figures S1,S2 and Tables S2,S3).[13]

The turnover frequencies (TOF) of 4-McyOH dehydration at 150°C on all MFI zeolites are compiled in Table 1. The highest TOFs appeared on zeolites (MFI-40 and MFI-60) with BAS concentrations of 0.23–0.31 mmol g⁻¹ and ionic strengths of 1.51–2.07 mol L⁻¹, respectively. Figure 1 A shows a volcano-shaped dependence of the TOF on the ionic strength. A similar trend is also seen when correlating the TOF with the
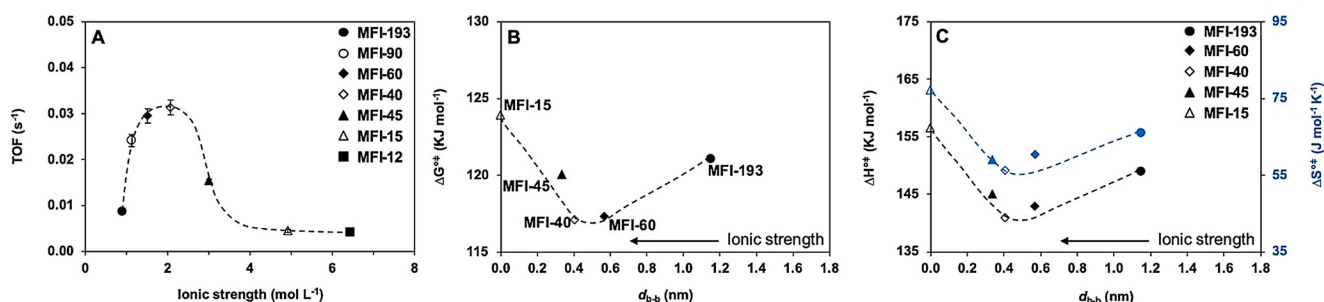
Figure 1. A) TOF as a function of ionic strength in the dehydration of 4-McyOH at 150°C. B) $\Delta G^{o\ddagger}$ and C) $\Delta H^{o\ddagger}$ (black) and $\Delta S^{o\ddagger}$ (blue) as a function of the distance between hydronium ions (d_{b-b}).

concentration of the hydrated hydronium ions ($H_3O^+_{hydr.}$) (Supporting Information, Figure S3). While for lower ionic strength a sharp increase of the TOF was observed, a decreasing trend is present for catalysts with high ionic strength. The volcano-shaped dependence of the TOF on the ionic strength was also consistently found at other reaction temperatures (160–190 °C, Supporting Information, Figure S4).

As we demonstrated previously,[12] the increasing local ionic strength in the zeolite pores causes the increase in TOFs. This conclusion was drawn unequivocally from a series of Na^+ partly exchanged H-MFI, in which the ionic strength was kept constant while at the same time the $H_3O^+_{hydr.}$ concentration was decreased.[12] Consequently, we conclude that also in the present study, the high ionic strength is responsible for the increasing TOFs by inducing non-ideality to the system. More precisely, the induced ionic environment destabilizes the uncharged sorbed reactant and simultaneously stabilizes the positively charged transition state (carbenium ion), which in turn results in an overall lowering of the free energy barrier and, therefore, in higher TOFs (Table 1).

The marked decrease of the TOF at very high ionic strengths, however, is hypothesized to result from reorganization of the ion pair by the spatial constraints brought by the neighboring $H_3O^+_{hydr.}$ to the organic substrate residing in between them. To explore this hypothesis, the distance between the boundaries of neighboring $H_3O^+_{hydr.}$ (d_{b-b}) in the investigated MFIs is plotted against the corresponding activation parameters (Figure 1 B and C). D_{b-b} is calculated by subtracting the length of a hydrated hydronium ion cluster consisting of eight water molecules $H^+(H_2O)_8$[10] from the distance between two centers of the clusters (d_{h-h})[16] (Figure 2 A), which is decreasing with decreasing Si/Al ratios and increasing $H_3O^+_{hydr.}$ concentrations, respectively (Figure 2 B). Figure 1 B illustrates that for the dehydration of 4-McyOH, $\Delta G^{o\ddagger}$ reaches a minimum at a d_{b-b} between 0.4 and 0.6 nm. For zeolites with smaller d_{b-b}, the free energy is increasing although featuring a higher ionic strength.

Once the void space between the hydronium ions is smaller than the volume of one substrate molecule, the repulsion induced by the sorption of molecules and the partial separation of charge via a rearrangement of the hydronium ions (combination of electrostatic, hydrogen bonding, and dispersion interactions) sets in in constrained systems forcing reorganization in the highly ionic strength environment.[12] The additional work resulting from the partial separation of the negative charge at the zeolite lattice and the positive charge (particularly for the transition state) that has to be overcome, causes an increase of the free energy and, therefore, a decrease of the TOF. In open systems[12] the TOF increased monotonically with increasing ionic strength without passing through a maximum. The sorption in the environment of higher ionic strength is compensated by volume expansion, which causes minimal additional work.
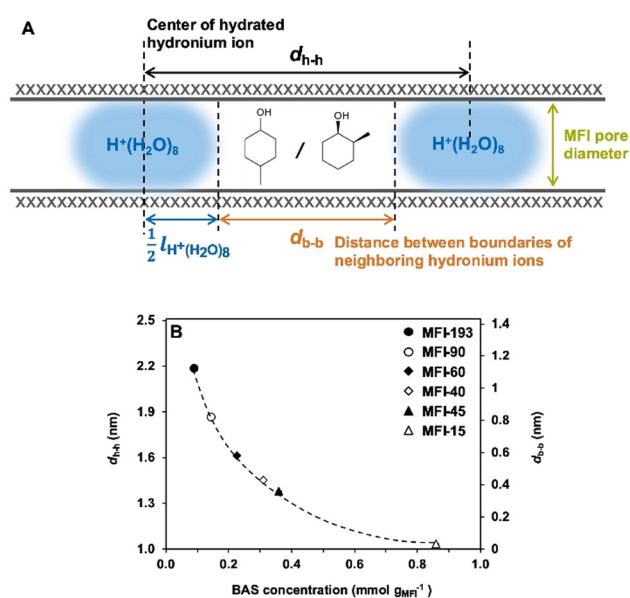

Figure 2. A) Illustration of the distance between the boundaries of neighboring hydronium ions (d_{b-b}) in the MFI pores adapted from reference 10. The distance between the centers of hydrated hydronium ions (d_{h-h}) is estimated by the cubic root of the average zeolite volume normalized to the number of hydronium ions.[10, 16] The $H^+(H_2O)_8$ cluster is assumed to be cylindric with the diameter of the H-MFI zeolite micropore channel.[17] B) D_{h-h} and d_{b-b} as function of the BAS concentration.

Alcohol adsorption measurements (Supporting Information, Figure S17, Table S16) confirm that the uptake of 4-McyOH starts to decrease on zeolites with ionic strength higher than 2 mol L^{-1}. However, it should be noted that the reaction is not transport limited despite steric constraints as also on these zeolites the reaction order in the alcohol was zero. In parallel with the variations of the free energy, the activation enthalpy and entropy obtained with the investigated MFI zeolites show an equal dependency on d_{b-b}. As soon as d_{b-b} falls below 0.4 nm, a sharp increase in $\Delta H^{o\ddagger}$ and $\Delta S^{o\ddagger}$ is observed. Despite the beneficial gain in entropy, the high enthalpic barrier more than offsets this contribution, resulting in the aforementioned increase in $\Delta G^{o\ddagger}$. Longer d_{b-b} again favor $\Delta S^{o\ddagger}$, but suffer from a lower stabilization of $\Delta H^{o\ddagger}$ than for zeolites with higher ionic strength.

The dehydration of *cis*-2-McyOH shows a similar volcano-shaped dependency of the TOF on the ionic strength and the BAS concentration, respectively (Table 2, Figure 3 A, Sup-

Table 2: Characterization of the investigated MFI zeolites, measured kinetic (150 °C) and activation parameters of *cis*-2-McyOH dehydration over MFI zeolites.

Entry	Zeolite	Ionic strength [mol L^{-1}]	TOF [s^{-1}]	$\Delta G^{o\ddagger}$ [kJ mol^{-1}]	$\Delta H^{o\ddagger}$ [kJ mol^{-1}]	$\Delta S^{o\ddagger}$ [J mol^{-1} K^{-1}]
1	MFI-193	0.89	0.019	118 ± 6	113 ± 3	−13 ± 7
2	MFI-60	1.51	0.076	114 ± 4	115 ± 2	2 ± 4
3	MFI-45	3.00	0.056	115 ± 7	111 ± 4	−10 ± 8
4	MFI-40	2.07	0.081	114 ± 6	114 ± 3	0 ± 7
5	MFI-15	4.92	0.045	116 ± 4	103 ± 2	−30 ± 4
6	MFI-12	6.44	0.021	119 ± 4	103 ± 2	−37 ± 4
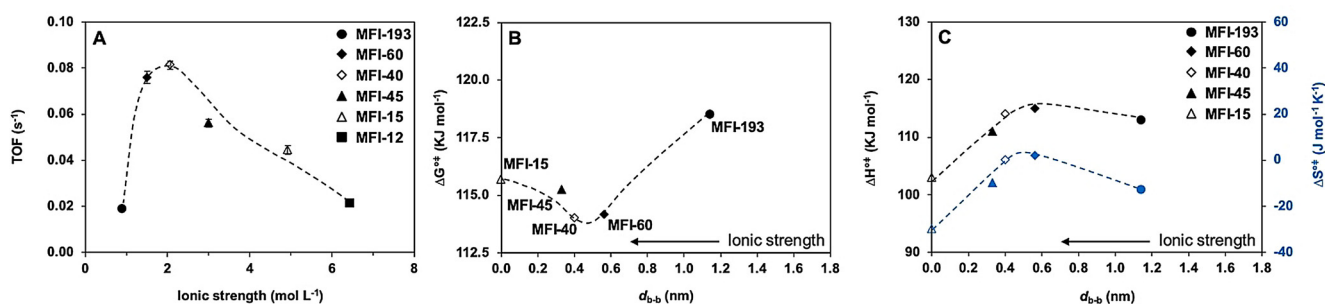
Figure 3. A) TOF as a function of ionic strength in dehydration of *cis*-2-McyOH at 150 °C. B) $\Delta G^{\circ\ddagger}$ and C) $\Delta H^{\circ\ddagger}$ (black) and $\Delta S^{\circ\ddagger}$ (blue) as a function of the distance between hydronium ions ($d_{b\text{-}b}$).

porting Information, Figure S3). The highest TOFs are again obtained at ionic strengths between 1.51–2.07 mol L^{-1}. As also in a concerted E2 dehydration pathway, the β-H abstraction (and simultaneous C−O bond cleavage) is the kinetically relevant step, the rate enhancement shows that also transition states in a concerted elimination benefit from a high ionic strength.

Interestingly, the drop of the reaction rates occurs at the symmetric situation as for 4-McyOH and prior for the non-substituted CyOH,[12] irrespective of the higher steric hindrance through the position and orientation of the substituted group or the mechanism pathway. $\Delta G^{\circ\ddagger}$ is increasing for all three substrates at the same boundary (Figure 1 B and 3 B), suggesting that the cyclohexyl ring determines the critical size (distance) after which the contribution of the repulsions exceeds the gain from the high local ionic strength. The reorganization penalty seems to have a less serve impact on the associated-complex than on the carbenium ion intermediate. This is demonstrated by the not as sharply decreasing volcano plot for the E2 compared to the E1 mechanism (TOF decrease from MFI-40 to MFI-45 ca. 31 % for E2 vs. ca. 52 % for E1).

Moreover, for the dehydration of *cis*-2-McyOH, the dependency of the activation enthalpy and entropy on $d_{b\text{-}b}$ shows an opposite trend (Figure 3 C). The enthalpic stabilization is now increasing for distances below 0.4 nm and above 0.6 nm, while a significant decrease of the entropy to negative values is observed. This loss in entropy is caused by the associated complex formed in the transition state of the concerted elimination consisting of a proton, the alcohol and water acting as the proton-abstracting base (Scheme 1).

The adsorption uptake of *cis*-2-McyOH is reduced, in line with the TOF decrease, after an ionic strength of 2.07 mol L^{-1} (Supporting Information, Figure S17, Table S16). This isomer showed an overall lower uptake than 4-McyOH due to its higher steric hindrance (on MFI-40: 0.34 mmol g^{-1} for *cis*-2-McyOH vs. 1.08 mmol g^{-1} for 4-McyOH). Nevertheless, the dehydration of *cis*-2-McyOH results in more than 2.5-fold higher TOFs (Table 1 and 3). As it was concluded previously, the antiperiplanar arrangement of the protonated hydroxyl group and the adjacent β-H allows the *cis*-2-McyOH to proceed via a concerted E2 mechanism, thereby resulting in an increased selectivity towards the energetically more favored Saytzeff-product (1-MCH) and simultaneously avoid-

ing the energetically demanding formation of a carbenium ion (Supporting Information, Table S17).[13]

Figure 4 displays that all tested zeolites follow a linear correlation between the entropy and enthalpy. Remarkably, the correlation even falls on the same line as all other secondary alcohols converted over various catalysts as reported recently.[18] This reflects the significant influence of the position of the OH-group on the overall catalytic activity (Supporting Information, Figure S18).
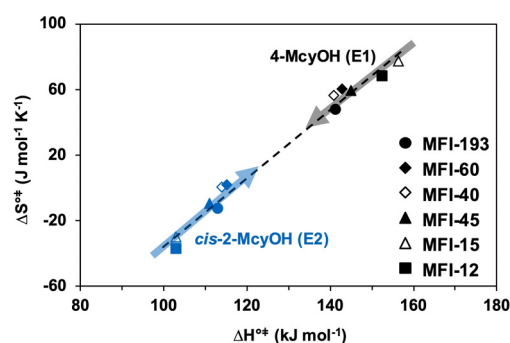

Figure 4. Correlation of the activation entropy ($\Delta S^{\circ\ddagger}$) and enthalpy ($\Delta H^{\circ\ddagger}$) in the dehydration of 4-McyOH (E1, black) and *cis*-2-McyOH (E2, blue).

Furthermore, Figure 4 highlights again that an increasing ionic strength has a different influence on the enthalpy and entropy when following an E1 or E2 mechanism. While a pronounced stabilization of $\Delta H^{\circ\ddagger}$ is characteristic for the E2 mechanism (absence of a carbenium ion), this pathway suffers from low or even negative $\Delta S^{\circ\ddagger}$ due to a highly ordered and multicomponent transition state. An increasing ionic strength has, in this case, a stronger beneficial impact on the entropy and shifts the parameters towards a more E1-like character (Figure 4, blue arrow). In contrast, an increasing ionic strength seems to shift an E1 mechanism more towards E2-like parameters by reducing the characteristic high enthalpic barrier at the expense of a lowering in entropy (Figure 4, black arrow).

In conclusion, we investigated the impact of the concentration of H$_3$O$^+$$_{\text{hydr.}}$ and the intracrystalline ionic strength on the aqueous phase dehydration of 2- and 4-methylcyclohex-anol. The increase of the turnover frequency in the demonstrated volcano plot is caused by increasing local ionic

strength in the zeolite pores. The highest dehydration rates were obtained by zeolites of moderate Si/Al ratios, i.e., on MFI-40 and MFI-60. The decrease, on the other hand, is arising from the additional work to overcome the strong repulsions once the void space between neighboring hydronium ions falls below the critical distance of 0.4 nm and a reorganization of the ion pairs is required. The position of the maximum is consistently found regardless of the substitution or whether the dehydration proceeds via an E1 or E2 mechanism. The reaction pathway strongly affects the activation entropy and enthalpy and the mode by which they are influenced by the ionic strength. While the formation of the carbenium ion primarily resulted in an enthalpic stabilization at high ionic strength, the formation of the associated complex was mainly entropically supported. The significantly higher rates for the *cis*-2-McyOH over the 4-McyOH dehydration, despite the higher steric bulkiness, are a consequence of the E2 pathway and the selective conversion to the Saytzeff product.

Conflict of Interest

The authors declare no conflict of interest.

[1] a) W. O. Haag, R. M. Lago, P. B. Weisz, *Nature* **1984**, *309*, 589–591; b) W. O. Haag, *Stud. Surf. Sci. Catal.* **1994**, *84*, 1375–1394.

[2] V. B. Kazanskii, *Acc. Chem. Res.* **1991**, *24*, 379–383.

[3] R. Gounder, E. Iglesia, *J. Am. Chem. Soc.* **2009**, *131*, 1958–1971.

[4] A. Janda, A. T. Bell, *J. Am. Chem. Soc.* **2013**, *135*, 19193–19207.

[5] S. Schallmoser, T. Ikuno, M. Wagenhofer, R. Kolvenbach, G. Haller, M. Sanchez-Sanchez, J. A. Lercher, *J. Catal.* **2014**, *316*, 93–102.

[6] a) A. Vjunov, J. L. Fulton, D. M. Camaioni, J. Z. Hu, S. D. Burton, I. Arslan, J. A. Lercher, *Chem. Mater.* **2015**, *27*, 3533–3545; b) A. Vjunov, M. A. Derewinski, J. L. Fulton, D. M. Camaioni, J. A. Lercher, *J. Am. Chem. Soc.* **2015**, *137*, 10374–10382.

[7] a) W. Lutz, H. Toufar, R. Kurzhals, M. Suckow, *Adsorption* **2005**, *11*, 405–413; b) R. M. Ravenelle, F. Schüßler, A. D'Amico, N. Danilina, J. A. van Bokhoven, J. A. Lercher, C. W. Jones, C. J. Sievers, *Phys. Chem. C* **2010**, *114*, 19582–19595.

[8] a) Y. Liu, A. Vjunov, H. Shi, S. Eckstein, D. Camaioni, D. Mei, E. Baráth, J. A. Lercher, *Nat. Commun.* **2017**, *8*, 14113; b) H. Shi, S. Eckstein, A. Vjunov, D. M. Camaioni, J. A. Lercher, *Nat. Commun.* **2017**, *8*, 15442; c) C. Zhao, J. A. Lercher, *Angew. Chem. Int. Ed.* **2012**, *51*, 5935–5940; *Angew. Chem.* **2012**, *124*, 6037–6042.

[9] a) M. Eigen, *Angew. Chem. Int. Ed. Engl.* **1963**, *2*, 1–19; *Angew. Chem.* **1963**, *75*, 489–508; b) G. Zundel, *Angew. Chem. Int. Ed. Engl.Angew. Chem. Int. Ed.* **1969**, *8*, 499–509; *Angew. Chem.* **1969**, *81*, 507–518.

[10] S. Eckstein, P. H. Hintermeier, R. Zhao, E. Baráth, H. Shi, Y. Liu, J. A. Lercher, *Angew. Chem. Int. Ed.* **2019**, *58*, 3450–3455; *Angew. Chem.* **2019**, *131*, 3488–3493.

[11] S. Eckstein, P. H. Hintermeier, M. V. Olarte, Y. Liu, E. Baráth, J. A. Lercher, *J. Catal.* **2017**, *352*, 329–336.

[12] N. Pfriem, P. H. Hintermeier, S. Eckstein, S. Kim, Q. Liu, H. Shi, L. Milakovic, Y. Liu, G. L. Haller, E. Baráth, Y. Liu, J. A. Lercher, *Science* **2021**, *372*, 952–957.

[13] P. H. Hintermeier, S. Eckstein, D. Mei, M. V. Olarte, D. M. Camaioni, E. Baráth, J. A. Lercher, *ACS Catal.* **2017**, *7*, 7822–7829.

[14] A. Hofmann, *Justus Liebigs Ann. Chem.* **1851**, *79*, 11–39.

[15] A. Saytzeff, *Justus Liebigs Ann. Chem.* **1875**, *179*, 296–301.

[16] G. T. Kokotailo, S. L. Lawton, D. H. Olson, W. M. Meier, *Nature* **1978**, *272*, 437–438.

[17] D. H. Olson, G. T. Kokotailo, S. L. Lawton, W. M. Meier, *J. Phys. Chem.* **1981**, *85*, 2238–2243.

[18] L. Milakovic, P. H. Hintermeier, Q. Liu, H. Shi, Y. Liu, E. Baráth, J. A. Lercher, *J. Catal.* **2020**, *390*, 237–243.